

3-Dimensional Dusty Plasma in a Strong Magnetic Field: Observation of Rotating Dust Tori

Mangilal Choudhary,^{1, a)} Roman Bergert, Slobodan Mitic, and Markus H. Thoma

*I. Physikalisches Institut, Justus-Liebig Universitt Giessen, Henrich-Buff-Ring 16,
D 35392 Giessen, Germany*

The paper reports on the dynamics of a 3-dimensional dusty plasma in a strong magnetic field. An electrostatic potential well created by a conducting or non-conducting ring in the rf discharge confines the charged dust particles. In the absence of the magnetic field, dust grains exhibit a thermal motion about their equilibrium position. As the magnetic field crosses a threshold value ($B > 0.02$ T), the edge particles start to rotate and form a vortex in the vertical plane. At the same time, the central region particles either exhibit thermal motion or $E \times B$ motion in the horizontal plane. At $B > 0.15$ T, the central region dust grains start to rotate in the opposite direction resulting in a pair of counter-rotating vortices in the vertical plane. The characteristics of the vortex pair changes with increasing the strength of magnetic field ($B \sim 0.8$ T). At $B > 0.8$ T, dust grains exhibit very complex motion in the rotating torus. The angular frequency variation of rotating particles indicates a differential or sheared dust rotation in a vortex. The angular frequency increases with increasing the magnetic field from 0.05 T to 0.8 T. The ion drag force and dust charge gradient along with the E-field are considered as possible energy source for driving the edge vortex flow and central region vortex motion, respectively. The directions of rotation also confirm the different energy sources responsible for the vortex motion.

^{a)}Electronic mail: Mangilal.Choudhary@exp1.physik.uni-giessen.de

I. INTRODUCTION

One of the characteristic features of a dusty plasma is the strong Coulomb interaction among the nearby negatively charged dust particles. The interaction strength determines its dynamical behavior to the external forces. Therefore, the investigation of the response of the dust grain medium to the external forces such as electrostatic force, neutral drag force, radiation pressure force, thermophoretic force, Lorentz force is of great interest¹. The external forces either affect the motion of dust grains directly or through the dynamics of the plasma species. External magnetic fields play a double role to control the dynamics of the dust grains, namely first through the Lorentz force acting on the plasma species (electrons and ions) and secondly through the Lorentz force acting on the dust particles. The motion of electrons and ions in the external magnetic field (B) affects the dust particles via the Coulomb collisions among them, which has been proven theoretically as well as experimentally²⁻⁴. However, the Lorentz force acting on the dust grains in the presence of a magnetic field needs to be explored in more detail.

In recent years, a lot of effort has been made to study the dust dynamics in the magnetized plasma background. Maemura *et al.*⁵ reported the transport of negatively charged particles in a DC discharge plasma when the applied magnetic field is perpendicular to the ambipolar electric field (E), which is a result of the $E \times B$ drift of the magnetized electrons. The role of the longitudinal magnetic field to the dust cluster confined in the electrostatic trap of the strata in a DC glow discharge has been studied in detail^{4,6-12}. In these studies, they observed the rotation of dust clusters about the discharge axis due to the $E \times B$ drift motion of ions. In a different DC discharge configuration, Sato *et al.*¹³ studied a volumetric or 3D dusty plasma in the presence of a magnetic field. They demonstrated the role of the coupling among the charged particles to establish the rotational motion in the magnetized plasma. Apart from DC discharges, a set of experiments have been performed in the magnetized RF discharges, where the RF sheath provides an electrostatic trap to the charged particles. The experiments of Konopka *et al.*¹⁴ and Huang *et al.*¹⁵ have demonstrated the role of the magnetic field on a 2D strongly coupled dust cluster, which exhibits a rigid and sheared rotation due to the $E \times B$ drift. The dynamics of a pair of grains in a planar 2D structure containing maximum 12 particles in the presence of a magnetic field has been studied by Cheung *et al.*¹⁶ and Ishihara *et al.*¹⁷. The dust cluster rotation is supposed to be based on

the $E \times B$ drift of the ions in the azimuthal direction of a cylindrical geometry. The azimuthal motion of ions transfers their momentum to the dust grains^{2,18}. The azimuthal motion of the neutral gas due to the drifted ions may also cause the dust rotation in the presence of a magnetic field^{19,20}. Instead of rotation, dust grains can also settle in the current filaments and show various kinds of patterns or ordered structures^{21,22} in the strong magnetic fields. All these studies were performed for a 2D dust cluster or 2D dusty plasma in the presence of an external magnetic field. Only limited work on the 3D dusty plasma is performed in magnetized DC and RF discharge plasmas^{13,23}. Saitou *et al.*²³ have observed the dynamic circulation of charged particles in a 3D dusty plasma in the presence of a magnetic field ($B \sim 0.2$ T). However, more work is needed to explore the dynamics of 3D dusty plasmas in a strong magnetic field and is the aim of the present investigation.

Section II deals with the detailed description of the experimental set-up and the plasma and dusty plasma production. The dynamics of a 3D dusty plasma confined by conducting and non-conducting rings is discussed in Section III. The origin of the observed vortex flow on the basis of available theoretical models is discussed in Section IV. A brief summary of the work along with concluding remarks is provided in Section V.

II. EXPERIMENTAL SETUP

Experiments are performed in an aluminium vacuum chamber, which is placed at the center of a superconducting electromagnet ($B_{max} \sim 4$ T) to introduce a homogeneous magnetic field in the plasma (or dusty plasma). The magnetized dusty plasma device which has been used in the present study is shown in Fig. 1(a). A schematic diagram of the experimental setup is presented in Fig.1(b). More details about the superconducting electromagnet can be found in ref²⁴. At first, the vacuum chamber is evacuated to base pressure $p < 10^{-2}$ Pa using a pumping system consisting of a rotary and turbo molecular pump. The experiments are performed with argon gas and the pressure inside the chamber is controlled by using a mass flow controller (MFC) and gate valve controller. For a given argon pressure, the plasma is ignited between an aluminium electrode of 65 mm diameter (lower electrode) and an indium tin oxide (ITO) coated electrode of 65 mm diameter (upper electrode) using a 13.56 MHz RF generator with a matching network. Both electrodes are separated by 30 mm and the upper transparent electrode is grounded along with the vacuum chamber. The

special design of the lower electrode, having a ring-shaped periphery with a height of 2 mm and width of 5 mm, provides a radial confinement to the negatively charged dust particles which are levitated above the lower electrode. An additional conducting (aluminium) or non-conducting (Teflon) ring is used to create a 3D dusty plasma in a strong magnetic field. It has been observed that dust grains without an additional confining ring are lost from central region to the edge of lower electrode in the case of strong magnetic fields ($B > 0.2$ T). Many rings of different diameters (30 mm to 8 mm) and heights (2 mm to 4 mm) are tested for the present study. We have found a suitable ring of inner diameter 10 mm, outer diameter 20 mm and height 4 mm to create a deep electrostatic potential well. Moreover, particle selection is also necessary to create a 3D dusty plasma at ground level experiments. Our primary measurements with different sized Melamine Formaldehyde (MF) particles suggest to use particles of radius, $r_d \simeq 1.7 \mu\text{m}$ to create an appropriate volume of dusty plasma. The vacuum chamber has 8 sides (or radial) ports. A dust dispenser, which is installed at one of the side ports of the vacuum chamber, is used for injecting the dust particles into the plasma. Two opposite side ports are used to observe the dusty plasma using a red laser and a CCD camera in the vertical plane. The CCD camera records images in the vertical plane (Y-Z plane) at 20 fps with a resolution of 1024×768 pixels. A CMOS camera is also installed to observe the dust dynamics through the transparent upper electrode in the horizontal plane (X-Y plane) at a frame rate of 90 fps and with a resolution of 2048×2048 pixels. A full view of the dusty plasma in the vertical (Y-Z) plane at $X = 0$ cm is shown in Fig. 2(a). Fig. 2(b) represents the dusty plasma view in the horizontal (X-Y) plane at $Z = 1.2$ cm. The stored images are analyzed with the help of ImageJ²⁵ software and MATLAB based open-access software, called openPIV²⁶.

III. DUST DYNAMICS IN THE PRESENCE OF MAGNETIC FIELD

The role of an external magnetic field on the dusty plasma has been explored by performing experiments using a conducting (aluminium) and non-conducting (Teflon) ring, which creates a deep and shallow potential well to confine the negatively charged dust particles. There are limitations to diagnose a large volume dusty plasma using the laser sheet, therefore, the dynamics of the dust grains in a vertical and horizontal plane are studied to understand the dynamics of the 3D dusty plasma. The detailed results are discussed in the

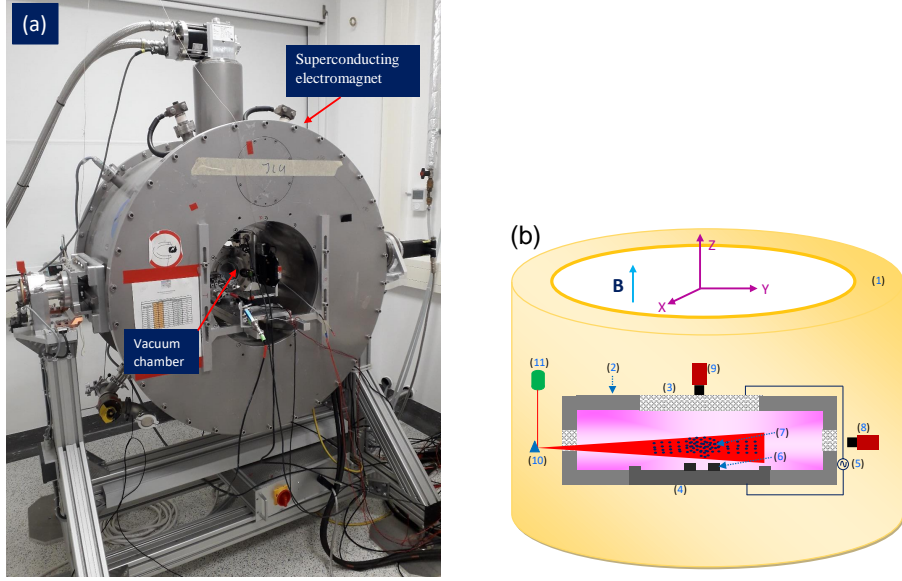


FIG. 1. (a) Magnetized Dusty Plasma Device at JLU. (b) Schematic diagram of the experimental setup for the dusty plasma study in a strong magnetic field. (1) Super conducting electromagnet, (2) vacuum chamber, (3) upper ITO coated transparent electrode, (4) lower aluminium electrode, (5) RF power generator, (6) aluminium or Teflon ring, (7) levitated dust particles, (8) CCD camera for vertical view, (9) CMOS camera for the horizontal view, (10) mirror, and (11) red laser with a cylindrical lens.

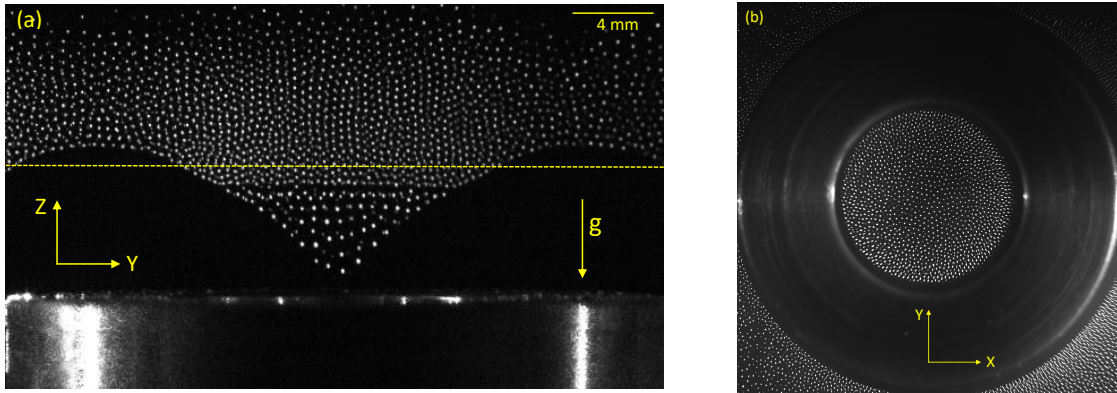


FIG. 2. (a) Full view of dusty plasma in a vertical plane ($Y-Z$) at the centre of the ring ($X = 0$ cm). (b) The horizontal view of the dusty plasma at the yellow dashed line (at $Z = 1.2$ cm) in Fig.2(a)

following subsection.

A. Dynamics of the dusty plasma confined by a conducting ring

An aluminium ring modifies the potential distribution in the sheath region of the lower electrode²⁷. It is known that charged particles follow the equipotential contour to achieve an equilibrium position. Therefore, particles are confined in a bowl shaped potential well created by the aluminium ring. Experiments are carried out at an argon pressure of $p = 35$ Pa and input rf power of $P = 3.5$ W. Fig. 3 shows the collective dynamics of the dusty plasma in the vertical (Y-Z plane) plane (at $X = 0$ cm) at various strengths of the external magnetic field. In this figure, all the images are reconstructed by the superimposition of five consecutive still images. The directed motion of dust grains forms elongated tracks, whereas the thermal motion of grains leaves white dots. In the absence of an external magnetic field, particles exhibit a thermal motion about their equilibrium position. As the magnetic field is increased up to 0.03 T ($B > 0.02$ T), the edge particles start to rotate in the vertical plane and form a vortex structure (V-I) on either side of the ring edge. Due to the symmetry about $X = 0$ cm in this plane, we have focused on the left side of the vortex structure for further analysis. It is also observed that the central region particles exhibit either thermal motion or $E \times B$ motion in the X-Y plane (or in the azimuthal direction of the cylindrical coordinate), which will be discussed later. Further increase of the magnetic field $B > 0.15$ T leads to a reduction in the size of the edge vortex (V-I) (see Fig. 4) and a rotation of the central region particles in the opposite direction, forming a pair of counter-rotating vortices. At $B = 0.2$ T, particles in the edge vortex (V-I) and central region vortex (V-II) are observed to rotate in opposite directions and form a counter-rotating vortex pair in this plane. The characteristics (shape, size, angular velocity etc.) of the counter-rotating vortices changes with further increase of the magnetic field up to 0.8 T. At strong magnetic fields, $B > 0.8$ T, the volume or the dust layers decreases. Hence, the size of the central vortex (V-II) reduces and the particles also exhibit a complex vortex motion which is difficult to diagnose with 2D optical diagnostics. It is also noticed that the levitation height as well the dust cloud width decrease at higher magnetic fields, which is an indication of the reduction of the sheath region.

To investigate the details of the velocity distribution and angular frequency (ω) of rotating

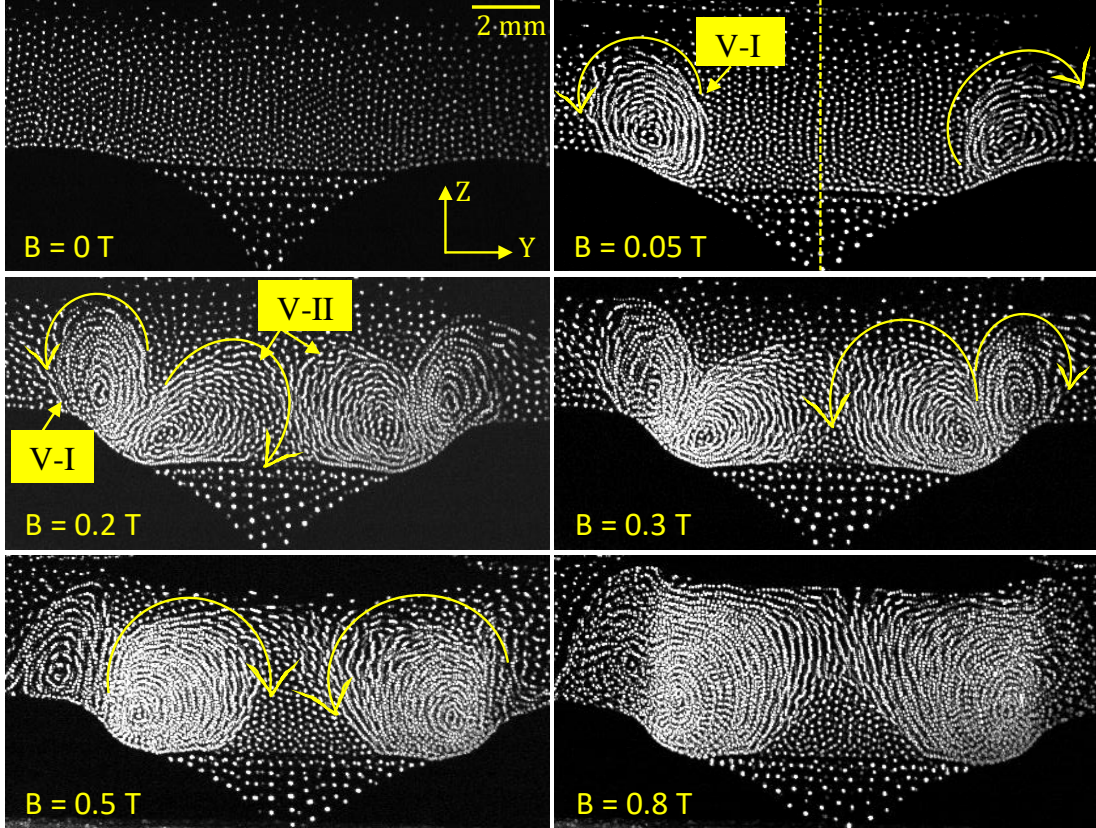


FIG. 3. Video images of the dust cloud in the vertical (Y - Z) plane at $X = 0$ cm. Images at different magnetic fields are obtained by a superposition of five consecutive images at a time interval of 65 ms. The edge vortex and central region vortex are represented by V-I and V-II, respectively. The vortex structures at different strengths of the magnetic field are observed at fixed input RF power, $P = 3.5$ W and argon pressure, $p = 35$ Pa. The dotted yellow line represents the axis of symmetry. The yellow solid line with an arrow indicates the direction of the vortex flow in the vertical plane of the 3D dusty plasma.

particles in a vortex structure the still images are analyzed using a MATLAB based open-access software, called openPIV²⁶ software. The PIV images of the dusty plasma in the vertical plane at different strengths of the magnetic field (see Fig. 3) are depicted in Fig. 5. These PIV images are constructed using an adaptive 2-pass algorithm (a 64×64 , 50% overlap followed by a 32×32 , 50% overlap analysis). The contour maps of the average magnitude of the velocities are constructed after averaging the velocity vectors of consecutive 50 frames. In the color map of the PIV images, the direction of the velocity vector represents the direction of rotating particles in the dust grain medium. Colour bars show the magnitude of

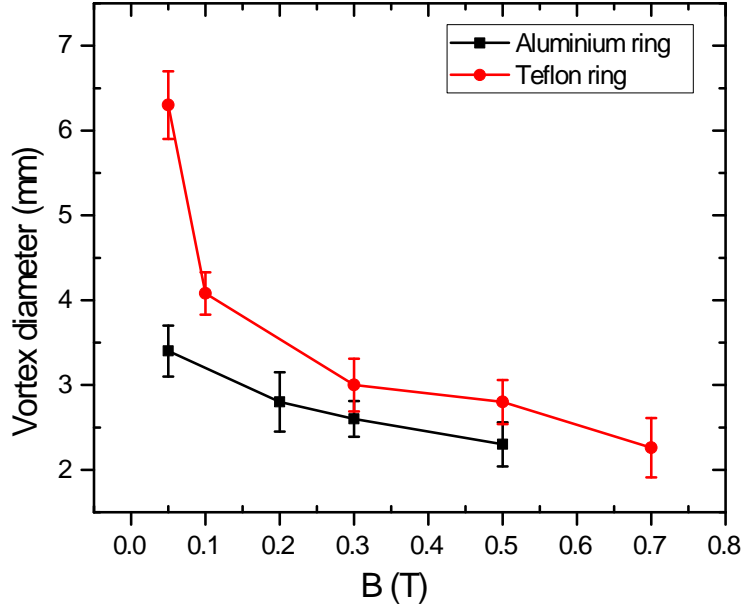


FIG. 4. Variation of the size of the edge vortex (V-I) depending on the external magnetic field strength.

the velocity distribution of rotating particles in the vortex structure. It is clear from Fig. 5 that the rotating particles have inhomogeneous velocity distribution in the vortex structure and the velocity of the rotating particles in either the edge vortex (V-I) or the central vortex (V-II) increases as the magnetic field is increased from 0.05 T to 0.8 T. To get the angular frequency, $\omega = v_t/\rho$, of the rotating particles in the edge vortex and central region vortex, different circular arc regions are analysed for different values of the magnetic field. Here v_t is the tangential velocity component and ρ is the radial distance from the center of a vortex. An average angular frequency of the rotating particles in the central region vortex (V-II) and the edge vortex (V-I) is presented in Fig. 6(a) and Fig. 6(b), respectively. It is clearly from fig. 6 that the angular frequency of the rotating particles decreases as the radial distance of the particles increases from the center of the vortex, $\rho = 0$ mm, for a given magnetic field. This is the signature of a differential or sheared rotation of the particles in the vortex. The angular frequency of the rotation increases with increasing external magnetic field at a given radial location from the center of the vortex, as shown in Fig. 6. It is also clear from figure 6 that the dust particles of the edge vortex (V-I) always have higher values of ω as compared to the central vortex (V-II) at a given value of the magnetic field.

For getting more information on the vortex flow in a 3D dusty plasma, images of the

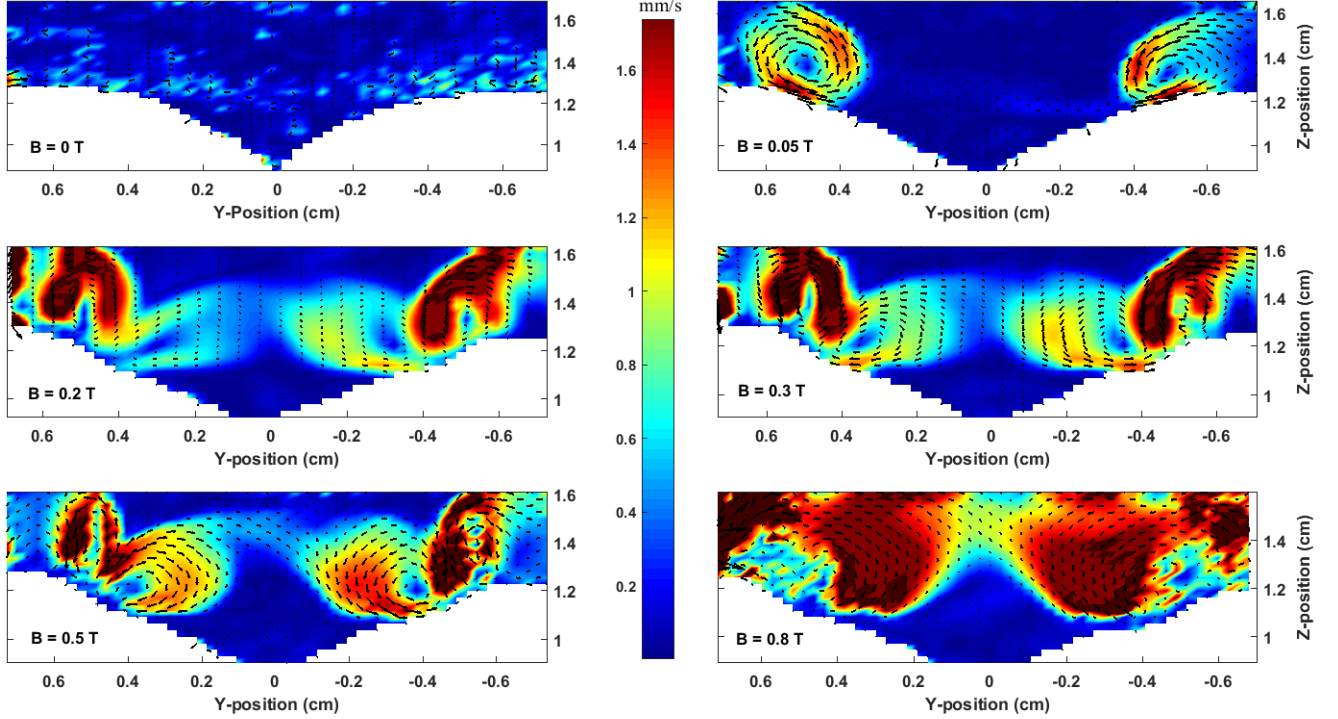


FIG. 5. PIV images of the corresponding video images of Fig. 3 at different magnetic field strengths in the vertical (Y-Z) plane. These images are constructed after averaging the velocity vectors over 50 frames. Arrows indicate the direction of rotation in a vortex and color bars represent the magnitude of the velocity of the rotating particles.

horizontal (or X-Y) plane are analyzed at different Z-positions. In Fig. 7, two PIV color map images of the dusty plasma at $Z \sim 1.5$ cm and $Z \sim 1.1$ cm in the presence of a magnetic field of $B = 0.4$ T are displayed. The direction of velocity vectors is outwards in Fig. 7(a) and inwards in Fig. 7(b), which corresponds to the edge vortex (V-I) and central region vortex (V-II), respectively. Now it is clear from figure 7 that the edge vortex and central region vortex in the Y-Z plane are cross sections of the rotating dust torus. A single vortex corresponds to a rotating dust torus. At higher magnetic fields, a pair of counter-rotating vortices in the Y-Z plane is nothing but a cross-section of a pair of counter-rotating tori in a dusty plasma. It is also observed that the velocity vectors have some angle to the radial direction (in the cylindrical coordinate) which suggest an $E \times B$ motion of the dust particles in the X-Y plane (or azimuthal direction) along with a rotational motion in the Y-Z plane. There may also be the possibility to have such kind of motion due to the dust-neutral collisions during the motion in the vertical plane. Therefore, the rotating dust particles in

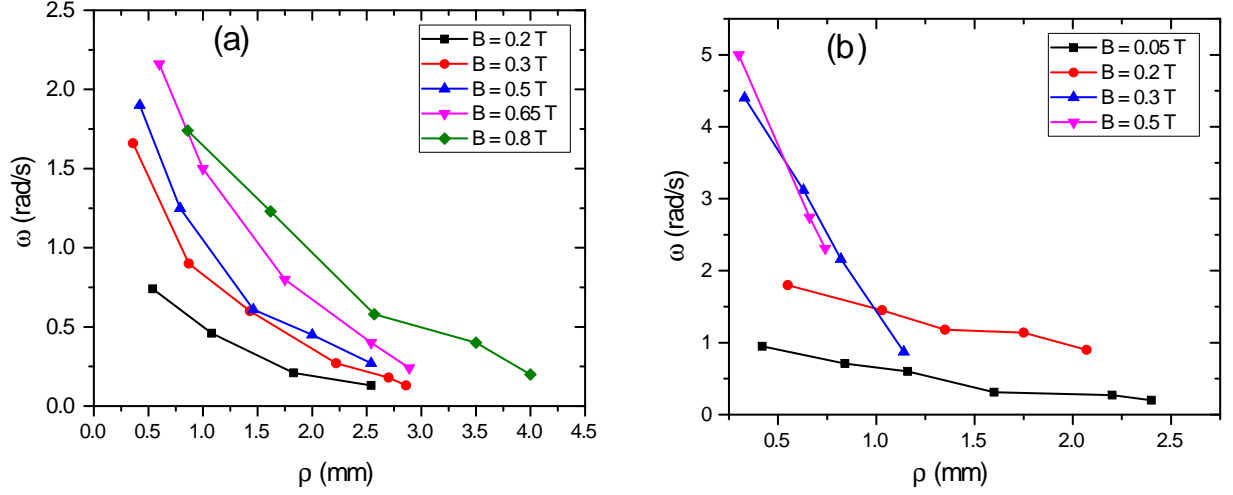


FIG. 6. The variation of the angular frequency of dust particles in the (a) central region vortex (V-II) and (b) edge vortex (V-I) at various strengths of the magnetic field. The error of the measured values are within $\pm 10\%$

Y-Z plane always have a drift in the azimuthal direction. It clearly indicates that particles do not rotate in a single Y-Z plane or a cross section of the dust torus but they shift to the next plane during the rotation. After a certain value of the magnetic field ($B > 0.5$ T), the rotating particles have a higher drift velocity (or azimuthal component) which is a signature of the helical type of motion in a dust torus. It is well known that the dust-dust interaction strength, which is termed as Coulomb coupling, is required to continue (or create) the vortex flow. In the case of weak coupling, dust grains do not show a collective response to external or internal forces. In our case, the particles levitated in the strong electric field of the sheath or the deep potential well (see Fig. 2(b)) seem to be weakly coupled because they do not participate in the vortex flow. These particles are acted upon by the ion drag force in the azimuthal or $E_r \times B$ direction and rotate in the horizontal plane, as shown in Fig. 8. Details about such a 2D dust rotation due to the $E \times B$ drift have been explained in earlier studies^{2,7,13,14}.

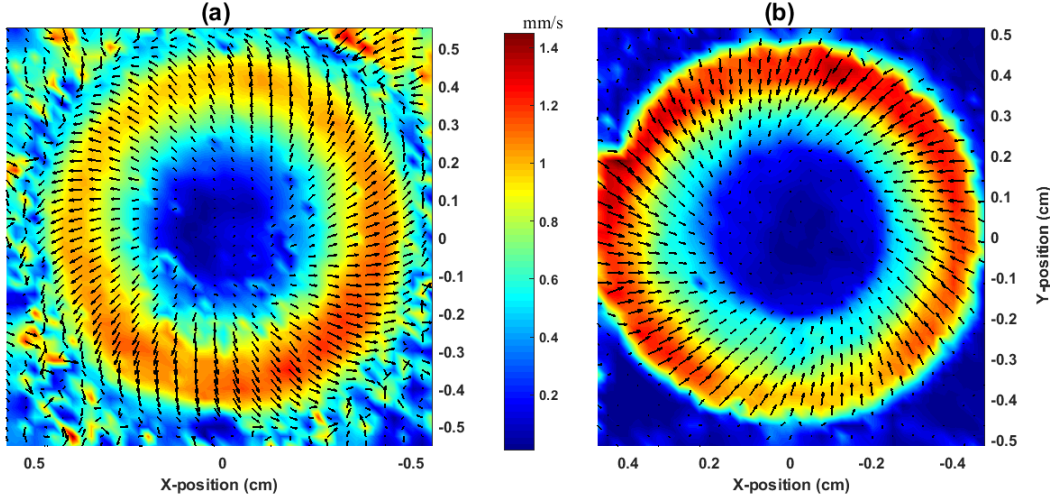


FIG. 7. (a) PIV velocity maps, constructed after averaging the velocity vectors over 50 frames in the horizontal (X–Y) plane at (a) $Z \sim 1.5$ cm and (b) $Z \sim 1.1$ cm in the presence of an external magnetic field of $B = 0.6$ T. The potential well is created by using the aluminium ring at argon pressure, $p = 35$ Pa and input RF power, $P = 3.5$ W.

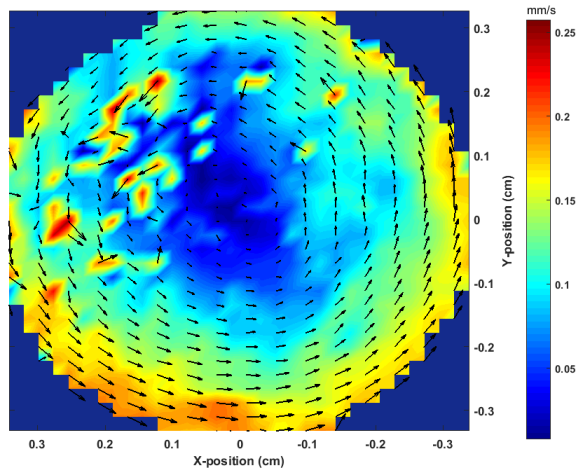


FIG. 8. PIV velocity maps, constructed after averaging the velocity vectors over 40 frames in the horizontal (X–Y) plane at $Z \sim 1$ cm in the presence of external magnetic field of $B = 0.2$ T. The potential well is created by using the aluminium ring at argon pressure, $p = 35$ Pa and input RF power, $P = 3.5$ W.

B. Dynamics of the dusty plasma confined by an insulating ring

In the previous subsection, dust grains were confined in a deep potential well above an aluminium ring, which has the same potential as the lower electrode. In the deep potential well, we have seen mixed motions of weakly and strongly coupled dust grains. Does the dusty plasma show a similar kind of motion when they are confined in a shallow potential well? Is it possible to get both phases of dusty plasma in shallow potential well? To answer these questions, a set of experiments is carried out in a dusty plasma which is confined by a non-conducting (Teflon) ring. Fig. 9 shows the dynamics of the dusty plasma created at argon pressure of $p = 35$ Pa and input RF power of $P = 3.5$ W in the presence of an external magnetic field. This figure is obtained after superimposing five consecutive images for tracking the motion of the dust particles. It is observed that the dust grains do not show any directed motion and exhibit only a thermal motion in the shallow potential in the absence of an external magnetic field ($B = 0$ T). The dust grains also exhibit only a thermal motion at low magnetic field ($B < 0.03$ T) and after that they start to rotate in this plane and form a pair of counter-rotating vortex structures at $B \sim 0.05$ T. With increasing magnetic field up to 0.1 T, we observe two well separated vortex structures at the edge of the potential well in this plane. Since the dusty plasma is symmetric about the X-axis in the Y-Z plane, we focus only on the left side region of the dust grain medium. The central region particles have a thermal as well as $E \times B$ motion in the X-Y plane. Increasing the magnetic field strength ($B > 0.15$ T), the dust grains in the central region start to rotate along with the edge vortex in opposite direction, resulting in a pair of counter-rotating vortex structures. Further increase in the magnetic field from 0.2 T to 0.7 T modifies the characteristics of this pair of counter-rotating vortices i.e. the size and velocity distribution of the particles in the vortices are changed. At $B \sim 0.7$ T, the central region vortex is shifted to the edge of the potential well and a well-separated pair of vortices is observed. At strong magnetic fields ($B > 0.7$ T), the dusty plasma volume reduces and only a few edge particles exhibit a vortex motion. As discussed before, the vortex structure in the vertical plane is a cross-section of the rotating dust torus. Hence at lower magnetic field a single rotating dust torus and a pair of counter-rotating dust tori at higher B is observed.

The earlier discussed PIV analysis technique is used to obtain the angular frequency distribution of rotating particles in a vortex structure at different magnetic field strengths.

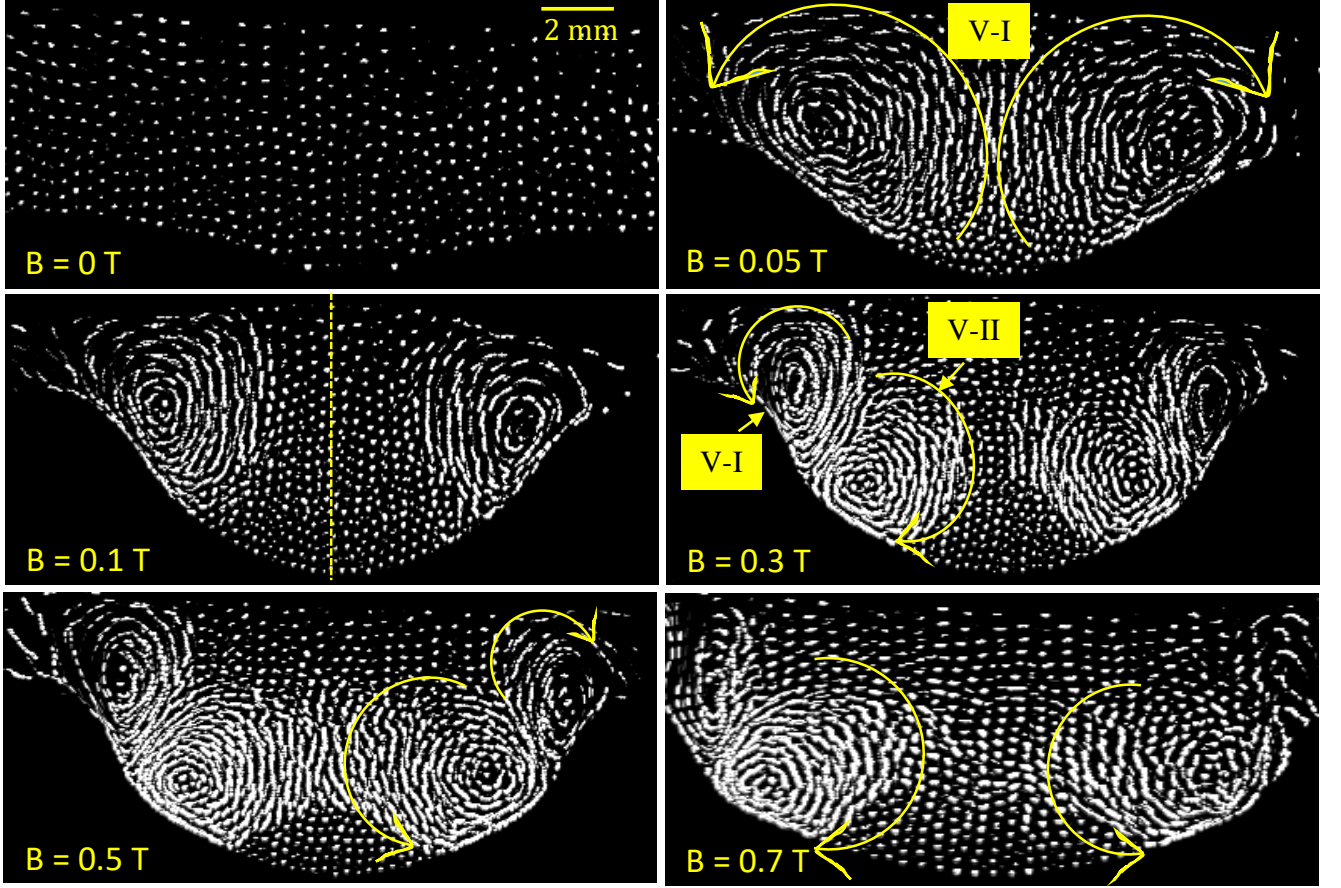


FIG. 9. Video images of the dust cloud in the vertical (Y-Z) plane at $X = 0$ cm. The images at different magnetic fields are obtained by a superposition of five consecutive images at a time interval of 65 ms. A Teflon ring is used to create a potential well at fixed input RF power, $P = 3.5$ W and argon pressure, $p = 35$ Pa. The yellow solid line with an arrow indicates the direction of vortex flow in the vertical plane of the 3D dusty plasma. V-I and V-II represent the edge vortex and central region vortex, respectively.

The average angular frequency of dust grains in the edge vortex (V-I) and central region vortex (V-II) is presented in Fig. 10(a) and Fig. 10(b), respectively. It is clear from Fig. 10 that the angular frequency ω decreases from the center to the outer edge of the vortices, which is a signature of the differential rotation. At given location of the vortex structure, the value of ω is observed to be higher at high magnetic field, showing the increase of ω with increasing external magnetic field. It is also clear from Fig. 10 that particles in the edge vortex always have a higher value of ω as compared to the central vortex at a given value of the magnetic field. Moreover, the particles confined in the potential well of the conducting

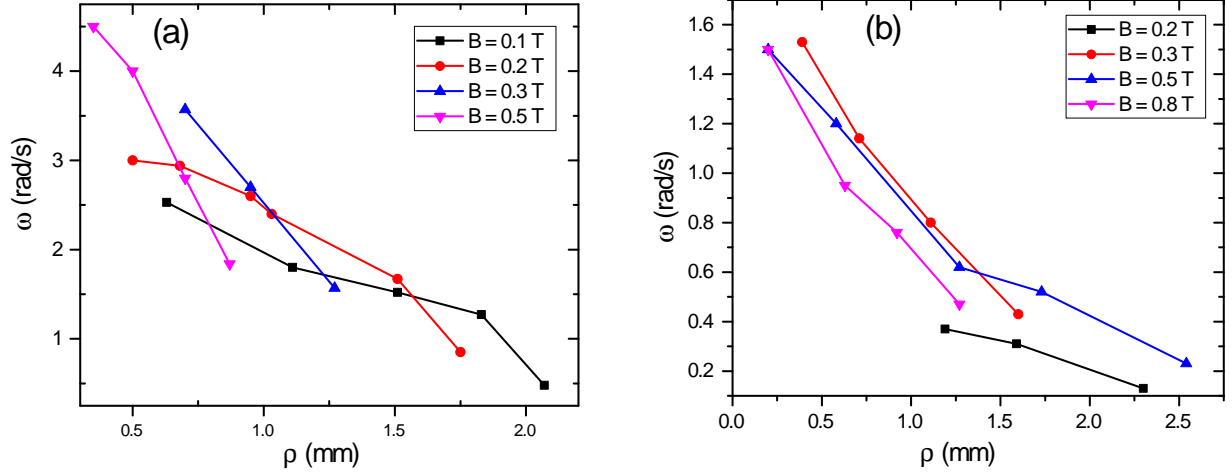


FIG. 10. Angular frequency variation of particles in (a) edge vortex (V-I) and (b) central region vortex (V-II) when the potential well is created a non-conducting (Teflon) ring at pressure, $p = 35$ Pa and RF power, $P = 3.5$ W. The error in the measured values of the angular frequency are within $\pm 10\%$

ring have a higher angular frequency than in the case of the non-conducting ring.

IV. DISCUSSION

The rotating dust grain medium in the external magnetic field can be described by the Navier-Stokes equation with the continuity equation of an incompressible fluid of constant mass density

$$\frac{d\vec{v}_d}{dt} = -\frac{1}{\rho}\nabla p + \eta\nabla^2\vec{v}_d + q_d(\vec{v}_d \times \vec{B}) + \frac{1}{m_d}(\vec{F}), \quad (1)$$

where

$$\vec{F} = \vec{F}_E + \vec{F}_g + \vec{F}_i + \vec{F}_n + \vec{F}_{th} \quad (2)$$

where $\rho = m_d n_d$ is dust mass density, n_d is the dust density, m_d is mass of the dust grain, η is the kinetic viscosity of the dust grain medium, and \vec{v}_d is the dust velocity. In the second equation, \vec{F}_E , \vec{F}_g , \vec{F}_i , \vec{F}_n , \vec{F}_{th} are the electrostatic force, gravitational force, ion-drag force, neutral drag force and thermophoretic force, respectively. The present set of experiments are carried out at an argon pressure of 35 Pa and the dust density n_d varies between 10^4 to 10^5 cm^{-3} . Therefore, the dust-neutral collision frequency ν_{dn} dominates over the dust-dust

collision frequency ν_{dd} . In such cases, the dust viscous force ($\eta\nabla^2\vec{v}_d$) is less dominant than the neutral drag force (F_n) for the dissipation loss during the steady vortex motion. For given discharge conditions and observed results, the Lorentz force on the dust grain is of the order of 10^{-18} to 10^{-20} N which is negligible compared to the external force F . The vortex motion in the dust grain medium can be described by the vorticity equation, which can be deduced from equation (1) after taking the curl of both sides²⁸

$$\frac{d\vec{\omega}}{dt} = \nabla \times \left[-\frac{1}{\rho}\nabla p + \frac{1}{m_d}(\vec{F}_E + \vec{F}_g + \vec{F}_i + \vec{F}_n + \vec{F}_{th}) \right], \quad (3)$$

where $\omega = \nabla \times \vec{v}_d$ is the vorticity of the rotating dust grain medium. Since the input power is low ($P = 3.5$ W), the role of thremophoretic force to the rotational motion is considered to be negligible. $\nabla \times \nabla p$ and $\nabla \times \vec{F}_g$ are zero, hence, equation (3) reduces to the form

$$\frac{d\vec{\omega}}{dt} = \frac{1}{m_d} \left(\nabla \times \vec{F}_E + \nabla \times \vec{F}_i + \nabla \times \vec{F}_n \right) \quad (4)$$

For the stationary two-dimensional (2D) vortices in a incompressible dusty plasma, equation (4) can be expressed as²⁸

$$\nabla \times \vec{F}_E + \nabla \times \vec{F}_i + \nabla \times \vec{F}_n = 0 \quad (5)$$

The electrostatic force on a dust grain of charge Q_d in the electric field of the sheath is given as $\vec{F}_E = Q_d\vec{E}$. Since ions are streaming in the direction of electric field, the ion drag force can be written as $F_i = F_i\hat{E}$. Here F_i represents the magnitude of the ion drag force on the dust grain. In the present set of experiments, there is no directed gas flow inside the chamber. Thus, neutrals provide a frictional background to resist the motion of the dust grains. According to Epstein friction²⁹, the neutral friction experienced by the dust grains is $\vec{F}_n = -m_d\nu_{dn}\vec{v}_d$. Here, ν_{dn} is the dust-neutral friction frequency. After substituting the values of these forces in equation (5), we get the following expression

$$\nabla Q_d \times \vec{E} + \nabla F_i(E) \times \hat{E} = m_d\nu_{dn}\nabla \times \vec{v}_d \quad (6)$$

In this equation, the L.H.S terms are the energy source for driving the vortex motion and the R.H.S term corresponds to the energy loss during the vortex motion. Thus, for maintaining a stationary vortex flow in the dusty plasma, the energy gain by particles must be balanced by the energy loss. It is clear from equation (5) that the charge gradient and ion drag gradient along with the electric field are possible energy sources to drive the vortex motion.

The charge gradient arises due to the inhomogeneity in the background plasma of the dust grain medium^{30,31}. For the ion drag force on the dust grain we take³²

$$\vec{F}_i = \frac{8}{3} \sqrt{2\pi k_B T_i M_i r_d^2 n_i} \left[1 + \frac{z\tau}{2} + \frac{z^2 \tau^2 \Lambda}{4} \right] (\vec{v}_i - \vec{v}_d) \quad (7)$$

where M_i , T_i , and n_i denote the mass, temperature and density of ions, respectively. $\vec{v}_i \gg \vec{v}_d$ is the average ion velocity (ion drift velocity), k_B is the Boltzmann constant, $z = Z_d e^2 / r_d T_e$ is the dimensionless charge of the dust particle, where Z_d is the dimensionless grain potential in units of T_e/e , $\tau = T_e/T_i$ is the electron-to-ion temperature ratio, and Λ is the modified Coulomb logarithm integrated over the ion velocity distribution function³². It is clear from equation (7) that the ion density and velocity are two major variables to determine the magnitude of ion drag force (F_i), hence, the ion drag gradient ($\nabla F_i(E)$) depends on n_i and v_i in the sheath region of the ring electrode.

In the absence of magnetic fields, the dust grains exhibit a thermal motion in the potential well (Fig. 2). The ion density and velocity gradient, which determine the magnitude of the ion drag gradient ($\nabla F_i(E)$) near the edge of the ring (or edge of the potential well), are not sufficient to drive the vortex flow. With the application of a magnetic field, the time-averaged electric potential distribution in the sheath region of the ring is modified which increases the radial electric field in the sheath region of the ring³³. At low magnetic field ($B < 0.2$ T) the plasma density or ion density increases due to the magnetization of electrons. The increase of the ion current to a cylindrical probe placed at the center as well as near to the edge of the ring (see Fig.11) is an indication of the ion density increment at low magnetic field. The radial electric field ($\vec{v}_i = \mu_i \vec{E}_r$) and ion density increase the radial ion shear flow driving the vortex flow in the presence of the electric field (E_z) against the dissipation loss by neutrals^{28,34,35}. The reduction in size of the modified potential distribution region³³ (or sheath region of ring electrode) directly relates to the size of the edge vortex. In our observations, we see a reduction in size of the edge vortex (see Fig. 4) which confirms the formation of a thin sheath or a higher electric field in the sheath of the ring. Thus. a higher magnetic field strength increases the ion drag gradient resulting in the formation of a vortex flow in the vertical plane or a rotating torus in the 3D dusty plasma. A schematic representation of the direction of the rotating particles due to the shear in the ion drag force along with electric field is shown in Fig. 12. In our experiments, the direction of the edge vortex flow (see Fig. 3 and Fig. 9) is found to be similar to that predicted by theory

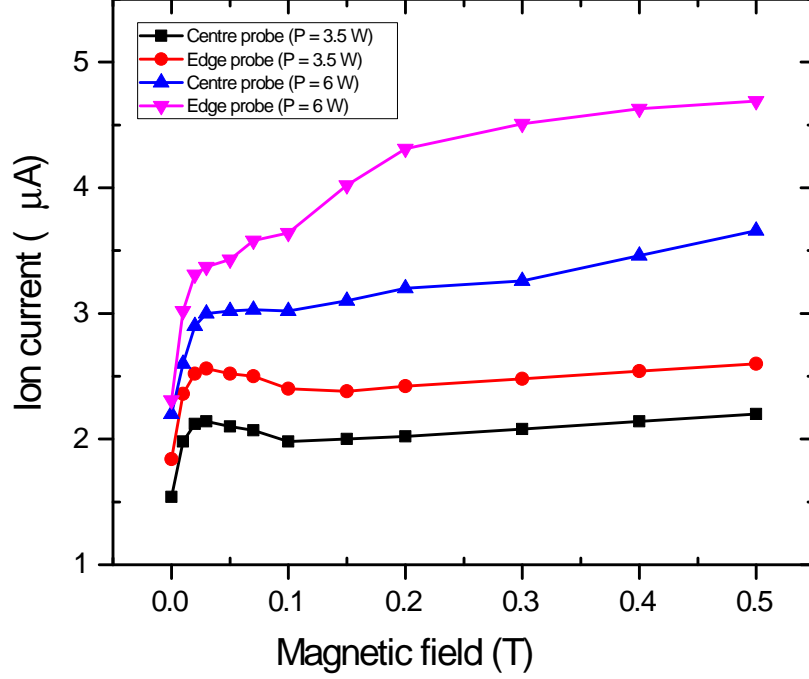


FIG. 11. Ion current measured by a cylindrical probe of length 3 mm and radius of 0.125 mm at the centre of ring and near to edge at different magnetic field strengths: The probe is kept at a fixed bias voltage of -30 V and the current is measured for powers of $P = 3.5$ W and 6 W at a pressure of $p = 35$ Pa. The errors in the measured values are within $\pm 5\%$.

which confirms the role of the ion drag gradient or ion shear flow along with electric field for creating the edge vortex (or dust torus).

The magnitude of the driving force ($|\nabla F_i(E) \times \vec{E}_z|$) determines the angular frequency of the rotating particles in the dust torus, which strongly depends on the sheath potential profile (or external magnetic field). Therefore, ω increases with increasing the strength of the external magnetic field.

The radial component of the electric field (E_r) in the presence of the magnetic field also drives an azimuthal drift flow of the ions through the $E \times B$ drift. These drifted ions in the azimuthal direction transfer momentum to dust particles and set them into rotational motion^{13,14,17}. This is one of the possible reasons for rotating dust grains moving in the next vertical plane. In the case of the conducting ring electrode, particles which are confined in the deep sheath region or bottom of the potential well are assumed to be less strongly coupled. We assume that these particles are either a result of agglomeration of particles or the presence of some massive impurity particles in the sample of mono-dispersive MF

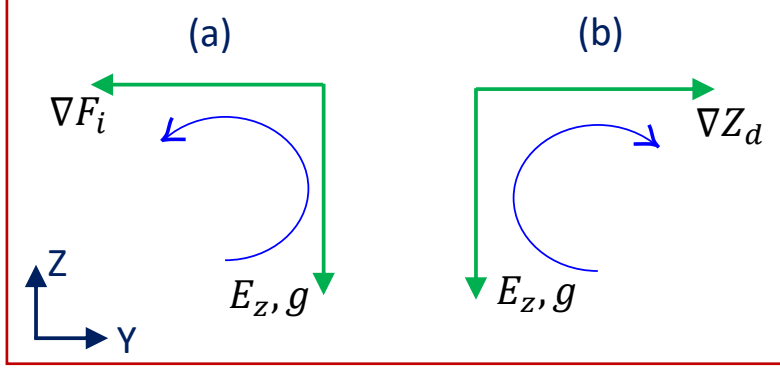


FIG. 12. Schematic representation of the rotational direction of particles caused by driving forces due to the ion shear flow and dust charge gradient.

particles. They do not participate in the vortex motion leading to a dust torus. These particles rotate in the azimuthal direction in the X–Y plane, which can be seen in Fig. 8.

At the higher magnetic field, $B > 0.15$ T the dust grains in the central region rotate in opposite direction to the edge vortex flow and form a pair of counter-rotating dust vortices (or dust tori). Does the ion shear flow along with electric field (E_z) drive the central region vortex motion? This is only possible if an opposite ion drag gradient builds up in the dusty plasma from the edge to the central region. The second possible source for driving a vortex flow in the opposite direction is a dust charge gradient along the electric field^{30,31,36–39}. Since the charge on dust grains is effectively determined by the magnitude of the electron and ion currents to their surface⁴⁰, spatial variation of the plasma parameters in the background plasma gives rise to a dust charge gradient. To characterize the background plasma of the dust grain medium in the presence of strong magnetic fields is a challenging task. Electrostatic probes, as well as spectroscopy, does not give reliable results, therefore, we tried to understand the observed results qualitatively based on the direction of the rotation and the ion current variation in the absence of dust particles which suggest the dust charge gradient as possible energy source to drive the central vortex flow (V–II). Below we explain the role of the magnetic field to drive the central vortex flow.

At $B > 0.15$ T, ions start to be magnetized and electrons are fully magnetized. The magnetic field reduces the plasma loss to the ring electrode, hence, the density of the plasma confined in the ring electrode increases. Increase in the ion current to a cylindrical probe

placed at center as well as near to edge of the ring indicates the increase in plasma density at higher magnetic field (see Fig.11). It has been demonstrated in simulation⁴¹ that ion current in the presence of magnetic field falls below the unmagnetized value if the ionization due to B is ignored. In our experiments, we also observe the either reduction of ion current or nearly constant between $B \sim 0.04$ to 0.15 T (see 11) due to less effect of B on ionization processes. After $B > 0.12$ T, the increase in ion current at given discharge condition is a signature of the plasma density enhancement. In the experiment, the glow intensity of the ring confined plasma is observed to increase in the strong magnetic field regime. The plasma glow and ion current variation towards higher magnetic field indicate the increase in the ion density. The density is expected to be larger near the edge of the ring and less towards the center of the ring, which is seen in Fig.11. Since ions are not drifting in the opposite radial direction, therefore, the role of ion shear flow to excite the rotational motion is assumed to be less dominant than the dust charge gradient. The grain charge is determined by the balance of electrons and ions flux to its surface⁴⁰. A reduction of the electron flux makes its surface less negative but, on the other hand, a smaller ion flux makes its surface more negative⁴². There are two possible mechanisms to create a spatial dust charge variation in the radial direction. First, the dusty plasma has a higher ion density near the edge of the ring, where the dust grains may collect more ions than at the central region where the ion density is less. Secondly, the electron temperature is expected to be lower near the edge than in the central region due to the electron density variation, hence, edge dust grains get less negative charges than the central region particles. Due to these both mechanisms, a spatial variation in the dust charge may develop from edge to center of the ring. This dust charge gradient $\nabla Q_d = e\nabla Z_d$, orthogonal to the gravitational force (\vec{F}_g), or ion drag force (\vec{F}_I) acting on the dust particles drive the vortex flow in the dust grain medium^{30,31,36-39}. With increasing magnetic field from 0.2 T to 0.8 T, the angular frequency of the rotating particles in the central region vortex (V-II) increases. This directly relates the magnetic field to the magnitude of the dust charge gradient or plasma density gradient. The direction of the vortex flow is according to the available theoretical model and agrees with our qualitative description for the central vortex flow.

V. SUMMARY

The present work highlights the collective dynamics of a 3D dusty plasma in the presence of an external strong magnetic field. The 3D dusty plasma is created in a capacitively coupled discharge by placing an additional conducting or non-conducting ring of a specific diameter and width on the lower electrode. The observed results of the reported work are summarised as:

1. A 3D dusty plasma in a strong magnetic field can be created using an additional conducting or non-conducting ring of a particular diameter and width in an RF discharge.
2. The magnetic field deepens the confining potential well creating a gradient in the plasma density. Hence, the ion shear flow or ion drag gradient drives the vortex motion of the dust grains.
3. At higher magnetic fields ($B > 0.15$ T), ions are magnetized and their density increases in the potential well. To maintain quasi neutrality, the electron density also increases. Thus, the magnetic field creates an inhomogeneous plasma in the confining potential well for $B > 0.15$ T. The plasma inhomogeneity is responsible for the dust charge gradient, which along with the electric field drives the vortex motion.
4. The angular frequency has a radial dependence which suggests a differential or sheared rotational motion in the vortices.
5. The magnetic field enhances the angular frequency of the rotating particles in the vortex. Particles in the potential well of the conducting ring have a higher angular frequency than that of the non-conducting ring.

The formation of the edge vortex is discussed on the basis of a radial ion shear flow or ion drag gradient together with the electric field in the presence of an external magnetic field. Weakly coupled particles rotate in the azimuthal direction due to the $E \times B$ drift of the ions in this plane. The onset of the vortex motion of the central region particles at higher magnetic field is understood by the presence of a dust charge gradient along with the electric field. The direction of the rotational motion in the vortices also supports the qualitative description of the vortex formation in the presence of a magnetic field.

There are challenges to diagnose the dusty plasma in the presence of strong magnetic fields using electrostatic probes as well as spectroscopy. For getting a better understanding of the collective dynamics of strongly magnetized dusty plasmas, computer simulations for such plasma systems are necessary. In the future, we plan numerical simulations to understand the presented experimental results in more details.

ACKNOWLEDGEMENT

This work is supported by the Deutsche Forschungsgemeinschaft (DFG).

REFERENCES

- ¹P. K. Shukla and A. A. Mamun, *Introduction to Dusty Plasma Physics*, series in plasma physics (IOP, Bristol, 2002).
- ²P. K. Kaw, K. Nishikawa, and N. Sato, “Rotation in collisional strongly coupled dusty plasmas in a magnetic field,” *Physics of Plasmas* **9**, 387–390 (2002).
- ³S. Nunomura, N. Ohno, and S. Takamura, “Effects of ion flow by $e \times b$ drift on dust particle behavior in magnetized cylindrical electron cyclotron resonance plasmas,” *Japanese Journal of Applied Physics* **36**, 877 (1997).
- ⁴E. S. Dzljeva, L. G. Dyachkov, L. A. Novikov, S. I. Pavlov, and V. Y. Karasev, “Complex plasma in glow discharge in a strong magnetic field,” *EPL (Europhysics Letters)* **123**, 15001 (2018).
- ⁵Y. Maemura, S.-C. Yang, and H. Fujiyama, “Transport of negatively charged particles by $e \times b$ drift in silane plasmas,” *Surface and Coatings Technology* **98**, 1351–1358 (1998).
- ⁶M. M. Vasiliev, L. G. Dyachkov, S. N. Antipov, R. Huijink, O. F. Petrov, and V. E. Fortov, “Dynamics of dust structures in a dc discharge under action of axial magnetic field,” *EPL (Europhysics Letters)* **93**, 15001 (2011).
- ⁷M. M. Vasil’ev, L. G. D’yachkov, S. N. Antipov, O. F. Petrov, and V. E. Fortov, “Dusty plasma structures in magnetic fields in a dc discharge,” *JETP Letters* **86**, 358–363 (2007).
- ⁸V. Y. Karasev, E. S. Dzljeva, A. Y. Ivanov, and A. I. Eikhvald, “Rotational motion of dusty structures in glow discharge in longitudinal magnetic field,” *Phys. Rev. E* **74**, 066403 (2006).

- ⁹A. R. Abdirakhmanov, M. K. Dosbolayev, and T. S. Ramazanov, “The gas discharge dusty plasma in a uniform magnetic field,” *AIP Conference Proceedings* **1925**, 020007 (2018).
- ¹⁰L. G. D’yachkov, O. F. Petrov, and V. E. Fortov, “Dusty plasma structures in magnetic dc discharges,” *Contributions to Plasma Physics* **49**, 134–147 (2009).
- ¹¹E. S. Dзлиeva, V. Y. Karasev, and A. I. Éikhval’d, “The onset of rotational motion of dusty plasma structures in strata of a glow discharge in a magnetic field,” *Optics and Spectroscopy* **100**, 456–462 (2006).
- ¹²V. Karasev, E. Dзлиeva, S. Pavlov, L. Novikov, and S. Maiorov, “The rotation of complex plasmas in a stratified glow discharge in the strong magnetic field,” *IEEE Transactions on Plasma Science* **46**, 727–730 (2018).
- ¹³N. Sato, G. Uchida, T. Kaneko, S. Shimizu, and S. Iizuka, “Dynamics of fine particles in magnetized plasmas,” *Phys. Plasmas* **8**, 1786–1790 (2001).
- ¹⁴U. Konopka, D. Samsonov, A. V. Ivlev, J. Goree, V. Steinberg, and G. E. Morfill, “Rigid and differential plasma crystal rotation induced by magnetic fields,” *Phys. Rev. E* **61**, 1890–1898 (2000).
- ¹⁵F. Huang, Y. H. Liu, M. F. Ye, and L. Wang, “Influence of gas pressure on the structure and dynamics of dust rotation in magnetized dusty plasmas,” *Physica Scripta* **83**, 025502 (2011).
- ¹⁶F. Cheung, A. Samarian, and B. James, “The rotation of planar-2 to planar-12 dust clusters in an axial magnetic field,” *New Journal of Physics* **5**, 75–75 (2003).
- ¹⁷O. Ishihara, T. Kamimura, K. I. Hirose, and N. Sato, “Rotation of a two-dimensional coulomb cluster in a magnetic field,” *Phys. Rev. E* **66**, 046406 (2002).
- ¹⁸O. Ishihara and N. Sato, “On the rotation of a dust particulate in an ion flow in a magnetic field,” *IEEE Transactions on Plasma Science* **29**, 179–181 (2001).
- ¹⁹A. V. Nedospasov, “Motion of plasma-dust structures and gas in a magnetic field,” *Phys. Rev. E* **79**, 036401 (2009).
- ²⁰J. Carstensen, F. Greiner, L.-J. Hou, H. Maurer, and A. Piel, “Effect of neutral gas motion on the rotation of dust clusters in an axial magnetic field,” *Physics of Plasmas* **16**, 013702 (2009).
- ²¹M. Schwabe, U. Konopka, P. Bandyopadhyay, and G. E. Morfill, “Pattern formation in a complex plasma in high magnetic fields,” *Phys. Rev. Lett.* **106**, 215004 (2011).

- ²²E. Thomas, U. Konopka, R. L. Merlino, and M. Rosenberg, “Initial measurements of two- and three-dimensional ordering, waves, and plasma filamentation in the magnetized dusty plasma experiment,” *Physics of Plasmas* **23**, 055701 (2016).
- ²³Y. Saitou and O. Ishihara, “Dynamic circulation in a complex plasma,” *Phys. Rev. Lett.* **111**, 185003 (2013).
- ²⁴M. Choudhary, R. Berger, S. Mitic, and M. H. Thoma, “Comparative study of the surface potential of magnetic and non-magnetic spherical objects in a magnetized rf discharge plasma,” <https://arxiv.org/abs/1901.10955> (2019).
- ²⁵C. Schneider, W. Rasband, and K. Eliceiri, “Nih image to imagej: 25 years of image analysis,” *Nature Methods* **9**, 671–675 (2012).
- ²⁶A. Liberzon, R. Gurka, and Z. Taylor, “<http://www.openpiv.net/openpiv-matlab/>,” (2009).
- ²⁷L.-J. Hou, Y.-N. Wang, and Z. L. Mikovi, “Two-dimensional radio-frequency sheath dynamics over a nonflat electrode with perpendicular magnetic field,” *Physics of Plasmas* **11**, 4456–4461 (2004).
- ²⁸T. Bockwoldt, O. Arp, K. O. Menzel, and A. Piel, “On the origin of dust vortices in complex plasmas under microgravity conditions,” *Phys. Plasmas* **21**, 103703 (2014).
- ²⁹P. S. Epstein, “On the resistance experienced by spheres in their motion through gases,” *Phys. Rev.* **23**, 710–733 (1924).
- ³⁰M. Choudhary, S. Mukherjee, and P. Bandyopadhyay, “Experimental observation of self excited co-rotating multiple vortices in a dusty plasma with inhomogeneous plasma background,” *Phys. Plasmas* **24**, 033703 (2017).
- ³¹O. S. Vaulina, A. P. Nefedov, O. F. Petrov, and V. E. Samaryan, A. A. and Fortov, “Self-oscillations of macroparticles in the dust plasma of glow discharge,” *Journal of Experimental and Theoretical Physics* **93**, 1184–1189 (2001).
- ³²S. A. Khrapak, A. V. Ivlev, G. E. Morfill, and H. M. Thomas, “Ion drag force in complex plasmas,” *Phys. Rev. E* **66**, 046414 (2002).
- ³³Y.-N. Wang and L.-J. Hou, “Rotation of 2d finite dust coulomb clusters in magnetic field,” *Thin Solid Films* **506-507**, 647–651 (2006).
- ³⁴K.-B. Chai and P. M. Bellan, “Vortex motion of dust particles due to non-conservative ion drag force in a plasma,” *Physics of Plasmas* **23**, 023701 (2016).

- ³⁵M. Laishram, D. Sharma, and P. K. Kaw, “Dynamics of a confined dusty fluid in a sheared ion flow,” *Phys. Plasmas* **21**, 073703 (2014).
- ³⁶O. S. Vaulina, A. P. Nefedov, O. F. Petrov, and V. E. Fortov, “Instability of plasma-dust systems with a macroparticle charge gradient,” *Journal of Experimental and Theoretical Physics* **91**, 1147–1162 (2000).
- ³⁷O. S. Vaulina, A. A. Samarian, O. F. Petrov, B. W. James, and V. E. Fortov, “Self-excited motions in dusty plasmas with gradient of charge of macroparticles,” *New Journal of Physics* **5**, 82 (2003).
- ³⁸M. Choudhary, S. Mukherjee, and P. Bandyopadhyay, “Collective dynamics of large aspect ratio dusty plasma in an inhomogeneous plasma background: Formation of the co-rotating vortex series,” *Physics of Plasmas* **25**, 023704 (2018).
- ³⁹A. Samarian, O. Vaulina, W. Tsang, and B. W. James, “Formation of vertical and horizontal dust vortexes in an rf-discharge plasma,” *Physica Scripta* **T98**, 123–126 (2002).
- ⁴⁰A. Barkan, N. D’Angelo, and R. L. Merlino, “Charging of dust grains in a plasma,” *Phys. Rev. Lett.* **73**, 3093–3096 (1994).
- ⁴¹L. Patacchini and I. H. Hutchinson, “Ion-collecting sphere in a stationary, weakly magnetized plasma with finite shielding length,” *Plasma Physics and Controlled Fusion* **49**, 1719–1733 (2007).
- ⁴²D. Lange, “Floating surface potential of spherical dust grains in magnetized plasmas,” *Journal of Plasma Physics* **82**, 905820101 (2016).